Parallel thermodynamic analysis of duplexes on oligodeoxyribonucleotide microchips

Alexander V. Fotin[1,2,3,], Aleksei L. Drobyshev[1], Dmitri Y. Proudnikov[2], Alexander N. Perov[1] and Andrei D. Mirzabekov[1,2,3,*]

Joint Human Genome Program: [1]Engelhardt Institute of Molecular Biology, Russian Academy of Sciences, 117984 Moscow, Russia, [2]Argonne National Laboratory, Argonne, IL 60439, USA and [3]Moscow Institute of Physics and Technology, 141700 Dolgoprudny, Russia

ABSTRACT

A microchip method has been developed for massive and parallel thermodynamic analyses of DNA duplexes. Fluorescently labeled oligonucleotides were hybridized with oligonucleotides immobilized in the $100 \times 100 \times 20\ \mu m$ gel pads of the microchips. The equilibrium melting curves for all microchip duplexes were measured in real time in parallel for all microchip duplexes. Thermodynamic data for perfect and mismatched duplexes that were obtained using the microchip method directly correlated with data obtained in solution. Fluorescent labels or longer linkers between the gel and the oligonucleotides appeared to have no significant effect on duplex stability. Extending the immobilized oligonucleotides with a four-base mixture from the 3′-end or one or two universal bases (5-nitroindole) from the 3′- and/or 5′-end increased the stabilities of their duplexes. These extensions were applied to increase the stabilities of the duplexes formed with short oligonucleotides in microchips, to significantly lessen the differences in melting curves of the AT- and GC-rich duplexes, and to improve discrimination of perfect duplexes from those containing poorly recognized terminal mismatches. This study explored a way to increase the efficiency of sequencing by hybridization on oligonucleotide microchips.

INTRODUCTION

Arrays of oligonucleotides immobilized on different supports (oligonucleotide chips) have been developed by a number of groups (1–5) and have found application in DNA sequencing by hybridization (SBH), mutant diagnostics, gene expression analysis and identification of microorganisms (6–11). Our group has been developing a MicroArray of Gel-Immobilized Compounds on a chip (MAGIChip™) (2,6,12). The microarray, a microchip, is a glass slide containing polyacrylamide gel pads of $60 \times 60 \times 20\ \mu m$ or larger. The gel pads are separated from each other by a hydrophobic surface and have a high immobilization capacity,

enabling them to be used as an array of microtest tubes with volumes of 70 nl and more (13). Microchips containing immobilized oligonucleotides, DNA, and different proteins and antibodies have been manufactured and tested for various applications (12).

In this paper, we describe a new application of oligonucleotide microchips for massive and parallel thermodynamic analysis of DNA duplexes. The melting curves were measured simultaneously for duplexes formed with all gel-immobilized oligonucleotides upon their hybridization with fluorescently labeled oligonucleotides in solution. Because it is more like homogeneous liquid-phase reactions, hybridization in a gel is more suitable for thermodynamic measurements than heterogeneous solid-phase hybridization of glass- or membrane-immobilized oligonucleotides (3,4,7). Thermodynamic analysis has shown that the stabilities in a gel of perfect DNA duplexes and duplexes containing single mispairs are less than, but directly correlates with, the stabilities of these duplexes in solution.

A number of programs to decipher whole genomes, raises the need for simple, fast and inexpensive sequencing methods. Sequence analysis by the hybridization of DNA with generic oligonucleotide microchips containing, for example, the whole set of all possible 65 536 8mers or 1 048 576 10mers can be useful for these programs. Generic microchips can be applied for (i) comparing the sequences of similar genes and genomes, (ii) proofreading the sequences obtained by conventional methods, (iii) sequence analysis of DNA clones, (iv) mapping and upon proper development, (v) *de novo* sequencing. Rather than embark directly on expensive manufacturing of these large microchips, we produced a much smaller generic microchip containing 4096 6mers and tested its effectiveness for sequence analysis (Mirzabekov *et al.*, unpublished results). The microchip 6mers have essential shortcomings: low stabilities of 6 bp long duplexes, less reliable results because of difficulties discriminating terminal mismatches, and a wide variation in the stabilities of AT- and GC-rich duplexes. By means of a thermodynamic analysis, we demonstrate that adding a universal nucleotide containing 5-nitroindole (14) or a mixture of 4 nt, A+G+T+C (15), to one or both ends of 6mers compensates for these shortcomings. Such additions increase the stabilities of the 6mer duplexes by lengthening them to 7 or 8 bp duplexes, destabilize the terminal mismatches by converting them into internal
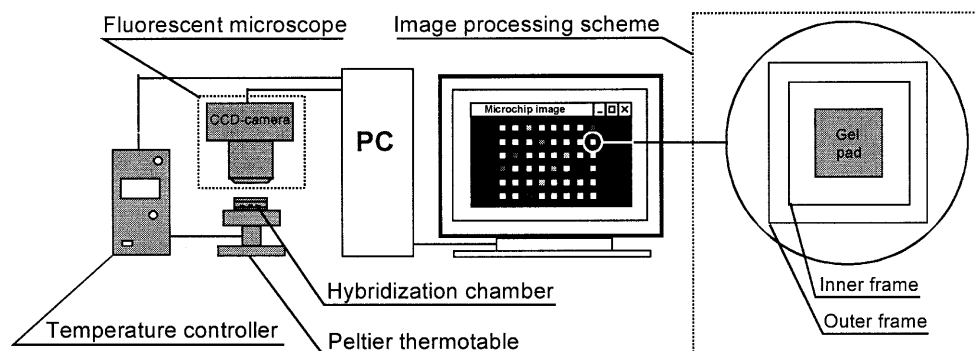

Figure 1. Experimental setup and image processing scheme.

ones, and can be used to equalize the stabilities of AT- and GC-rich duplexes. These results have formed the basis for the construction of a generic 6mer microchip.

MATERIALS AND METHODS

Oligodeoxyribonucleotides

3-Methyluridine controlled pore glass (CPG) was synthesized as described previously (16). 5-Nitroindole-CE Phosphoramidite (universal base), 3′-Amino-Modifier C7 CPG, Spacer Phosphoramidite 9 [tri(ethylene glycol) phosphoramidite] and dSpaser (1,2-dideoxyribose phosphoramidite) were purchased from Glen Research (Sterling, VA). HEX-phosphoramidite (hexachloro-fluorescein phosphoramidite, fluorescent label) was from Applied Biosystems (Foster City, CA).

Oligonucleotides were synthesized on an Applied Biosystems 394 DNA/RNA synthesizer, using standard phosphoramidite chemistry. 5-Carboxytetramethylrodamine succinimidyl ether (TMR, Molecular Probes Inc., Eugene, OR) was linked to the 3′-terminal amino group of oligonucleotides according to manufacturer's protocol.

Microchip manufacturing

Arrays of polyacrylamide gel pads of $100 \times 100 \times 20$ µm spaced by 200 µm, were prepared by a photopolymerization procedure (12). Oligonucleotides for immobilization were activated by oxidation of 2′,3′-cisdiol groups of 3′-terminal 3-methyluridine by $NaIO_4$. The gel was activated by partial substitution of amide groups with hydrazide (6). Spacers [1,2-dideoxyribose or tri(ethylene glycol)] were introduced between 3-methyluridine and some immobilized oligonucleotides. Droplets (0.3 nl) of activated oligonucleotides (100 µM) were applied to each gel pad.

Hybridization and melting

All experiments were performed in real time on an automatic experimental setup consisting of a two-wave-length fluorescent microscope, CCD-camera, Peltier thermotable, temperature controller and a computer equipped with a data acquisition board (Fig. 1). Special software was designed for experimental control and data processing, which used a LabVIEW virtual instrument interface (National Instruments, Austin, TX). All hybridizations were carried out in a hybridization chamber with a working volume of 15 µl. The total exposure time did not exceed 3 min (no more than 80 acquisitions during the timecourse of an experiment

were made with 1–2 s for a single measurement), which was far less than exposure time required for photobleaching of fluorescent labels (1 h for 30% loss of fluorescent intensity).

Hybridization of an octamer microchip containing oligo-nucleotides with 5′-terminal HEX labels (concentration 0.75–3.0 µM) was performed in a hybridization buffer of 1 M NaCl, 5 mM EDTA, 1% Tween and 10 mM $NaHPO_4$, pH 6.8. The hybridization chamber was cooled from +45 to –4°C at a rate of 0.5°C/min to measure the temperature dependence of the hybridization signal. In control experiments we raised the temperature from –4 to 40°C at the same rate and showed that both annealing and melting of the duplexes provided virtually coincident curves (Fig. 2A). The absence of hysteresis suggests that these curves were measured under equilibrium conditions; hence we refer to both of them as equilibrium melting curves.

The effect of duplex length on its stability was estimated by measuring the melting curves from –20 to +60°C in a hybridization buffer of 4.5 M NaCl, 5 mM EDTA, 1% Tween and 10 mM $NaHPO_4$, pH 6.8. Equilibrium melting curves in these experiments were registered at increasing temperature at a rate from 1°C/h at low temperatures (–20°C) to 1°C/2 min at high temperatures (+60°C). Time of equilibrium establishment was determined to be the time required for the hybridization signal to reach a plateau after the stepwise temperature change.

The total amount of labeled target oligonucleotides in hybridization solution varied in the different experiments from 7.5 up to 45 pmol, and was always much higher than the amount of immobilized oligonucleotides (~30 fmol per gel pad). Therefore, one can consider that concentration of labeled target remained constant during hybridization even when all the immobilized oligonucleotides are saturated.

Image processing and melting curve analysis

The excess of labeled oligonucleotides in solution creates a rather strong background during hybridization. The following algorithm for image analysis was developed to subtract this background from the hybridization signals. The 100×100 µm gel pads spaced 200 µm from each other were surrounded by two square frames: a 180×180 µm inner frame and a 230×230 µm outer frame (see Fig. 1, image processing scheme). The fluorescent signal was averaged inside the inner frame (C) and in the space between the inner and outer frames (B, background). The hybridization signal (J) from duplexes formed was obtained by subtracting background from the signal of the inner frame and dividing this value by background to compensate the temperature dependence of
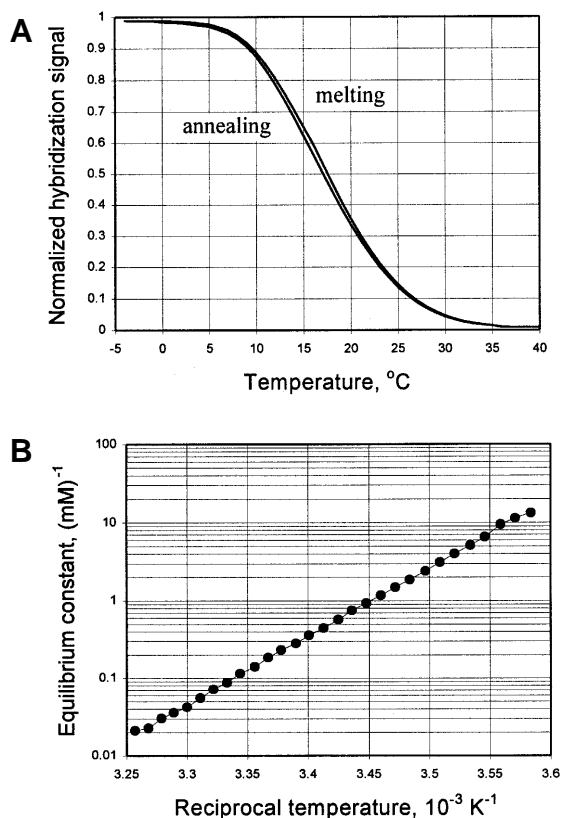
Figure 2. Hybridization of fluorescently labeled 13mer 5′-HEX-d(GTCCAGTC-CAATA) with a complementary microchip deoxy8mer, 3′-CAGGTCAG-5′ (underlined bases comprise the complementary region). (**A**) Melting and annealing curves. (**B**) Equilibrium constant versus reciprocal temperature. Linear dependence is obtained by fitting of the parameter *A* in Equation **2**.

fluorescence and the variations in intensity of exciting light, that is, *J = (C – B)/B*. We used inner frames larger than the gel pads to avoid occasional displacements of the microchip during the timecourse of the experiment. As can be seen, the size of both the frames can be chosen quite arbitrarily because the averaged values of the signals were used.

RESULTS AND DISCUSSION

Thermodynamic analysis of DNA duplexes on microchips

Hybridization of fluorescently labeled oligonucleotides in solution with the microchip-immobilized oligonucleotides was monitored quantitatively with a fluorescent microscope equipped with a CCD camera (6). The equilibrium melting curves of the duplexes were measured in parallel for all the microchip oligonucleotides in real time (1–2 s for a single acquisition) in a stepwise-increased temperature gradient. The thermodynamic parameters of the duplexes were calculated from the melting curves.

A typical equilibrium melting curve for a microchip 8 bp duplex is shown in Figure 2A. A fluorescently labeled 13mer present in solution in ~100-fold excess was hybridized with an immobilized 8mer. The classical equation for melting curve analysis (17) could not be applied in this case because it is valid only for equal concentrations of both strands. Consequently, we developed an alternative method for calculating the thermodynamic parameters from the melting curves of the microchip duplexes.

The equilibrium constant $K(T)$ may be expressed in terms of the concentration of free oligonucleotides, *f*, which is supposed to be constant; the concentration of immobilized oligonucleotides, *m*; and the concentration of bound oligonucleotides, *b(T)* as follows:

$$\frac{1}{K(T)} = f \times \left(\frac{m}{b(T)} - 1 \right) \qquad \textbf{1}$$

Because *b(T)* is proportional to the hybridization signal, *J(T)*, one can rewrite this equation as

$$\frac{1}{K(T)} = f \times \left(\frac{A}{J(T)} - 1 \right) \qquad \textbf{2}$$

where *A* is a constant proportional to the concentration of immobilized oligonucleotides, and should be fitted to obtain the linear dependence of *ln K* on reciprocal temperature according to the van't Hoff equation (17):

$$In \ \ K(T) = \frac{\Delta H}{RT} - \frac{\Delta S}{R} \qquad \textbf{3}$$

Figure 2B represents the dependence of the equilibrium constant on the reciprocal temperature as a result of the melting curve analysis. Enthalpy (ΔH) and entropy (ΔS) of the duplex melting can be calculated from the slope and intercept of this curve according to Equation **3**. The value of the equilibrium constant, *K*, at standard temperature (298°K) allows calculation of the standard transition free energy value ΔG^0 according to Equation **4**:

$$\Delta G° = -RT_0 \ ln[K(T_0)] \qquad \textbf{4}$$

where $T_0 = 298°K$.

The melting temperature, T_m, is usually defined as the midpoint of the melting transition, and depends on strand concentrations. When both strands are presented in equimolar ratio, the equilibrium constant at midpoint equals one half of the initial concentration of one strand (17). For comparative analysis of microchip and solution (18) data, we redefined the melting temperature as the temperature T_μ at which $K = 1 \ \mu M^{-1}$. Such calculations of the melting temperature are independent of strand concentrations and therefore allow the thermodynamic data obtained on microchips to be reliably compared with those obtained in solution. Since the initial concentration of oligonucleotides in solution was 2 μM (18), it is apparent that $T_\mu = T_m$ measured in solution.

Stabilities of perfect and mismatched duplexes in gel versus solution

Doktycz *et al*. measured thermodynamic parameters for a number of 8 bp long perfect (18) and mismatched (unpublished data) duplexes in solution. We compared the properties of some duplexes in solution with those in gel in our study.

Nine fluorescently labeled 13mers have the common structure of 5′-HEX-d(GTCCAGTCCAXYZ), where XYZ are ATA, AGA, GAA, TCA, CAT, TCC, GGG, CCG and CGC (underlined regions in 13mers are complementary to the microchip 8mers). The microchip contains 64 gel pads with immobilized deoxy8mers of the common structure of 3′-CAGGTX_1Y_1Z_1-5′, where X_1, Y_1 and Z_1 are A, T, G or C. Five 5′-terminal nucleotides are present to reduce the influence of the HEX label on the duplexes and to extend the constant region of the 13mer for hybridization with the complementary control deoxy8mer 3′-CAGGTCAG-5′ of the microchip.

Table 1. Thermodynamic parameters (ΔH, ΔS, ΔG^0 and T_μ) for deoxy8 bp duplexes measured on the microchips and in solution, as determined by Doktycz *et al.* (18), except where indicated

Duplex structure	ΔH, kcal/mol		ΔS, cal/mol·K		ΔG^0, kcal/mol		T_μ, °C	
	chip	solution	chip	solution	chip	solution	chip	solution
ATA/TAT	32	58	91	166	5.39	8.46	3	26.5
AGA/TCT	35	57	97	160	5.72	8.82	5	28.6
GAA/CTT	35	57	96	160	6.49	9.16	12	30.4
TCA/AGT	36	57	101	161	6.31	9.46	12	31.9
CAT/GTA	32	58	84	161	6.52	9.71	11	33.2
TCC/AGG	38	60	105	167	6.52	10.23	13	35.4
GGG/CCC	34	61	89	169	7.47	10.81	20	38.5
CCG/GGC	32	63	80	173	8.27	11.31	26	40.8
CGC/GCG	34	66	87	181	8.05	12.13	24	44.0
GTC/CAG	38	64	97	181	7.22	9.99	17	33.8
GAa/CTg[a]	30	44	81	119	5.61	8.56	7	27.2
GAa/CTa[a]	32	49	88	133	5.68	8.60	8	28.1

[a]Values given are taken from the unpublished data of Doktycz *et al.* (18).
Parameters were recalculated to be relevant to standard conditions [$\Delta G^0 = 0$ when $K = 1$ M^{-1}, rather than 1 µM^{-1} as in Doktycz *et al.* (18)]. Microchip nine deoxy8 bp perfect duplexes (nos 1–9) and two duplexes containing terminal a–g and a–a mispairs (nos 11,12) were formed by the hybridization of labeled 13mers, 5′-HEX-d(GTCCA<u>GTCCAX-YZ</u>), in solution with immobilized 8mers, 3′-gel-<u>CAGGTX$_1$Y$_1$Z$_1$</u>-5′. The structure of the tenth deoxy8 bp duplex, used as a control, is 5′-HEX-d(<u>GTCCAGTCCAX-YZ</u>)/3′-gel-<u>CAGGTCAG</u>-5′. The variable parts 5′-XYZ-3′/3′-X$_1$Y$_1$Z$_1$-5′ are presented in the first column. The complementary regions in the oligonucleotides are underlined. Mispairs are marked in low cases. The margin of error for the microchip data is 5% for ΔH and ΔS, 0.05 kcal/mol for ΔG^0 and 0.5°C for T_μ.

The thermodynamic data for 12 different 8 bp microchip duplexes, both perfect and containing terminal a–g and a–a mispairs, as well as for the same duplexes in solution, are summarized in Table 1. The terminal mismatches, as expected, have a rather low destabilizing effect on the duplexes. The data presented are the average of three experiments performed on different microchips. The root mean square deviations for the fitting procedure lead to a 5% margin of error in ΔH and ΔS, 0.05 kcal/mol in ΔG^0 and 0.5°C in T_μ. Figure 3A and B shows the plots of ΔG^0 and T_μ measured on microchips against those obtained in solution and recalculated to be relevant to standard conditions [$\Delta G^0 = 0$ when $K = 1$ M^{-1}, rather than 1 µM^{-1} as in Doktycz (18)]. The data from Figure 3A reveal the linear trend:

$$\Delta G^0(\text{microchip}) = a\Delta G^0(\text{solution}) + g, \qquad \mathbf{5}$$

where $a = 1.1 \pm 0.2$ and $g = -3.2 \pm 0.4$ kcal/mol. Or, assuming that $a = 1$:

$$\Delta G^0(\text{microchip}) = \Delta G^0(\text{solution}) - (3.2 \pm 0.4) \text{ kcal/mol.} \quad \mathbf{6}$$

The best linear fit for plots of T_μ for the microchips versus solution is:

$$T_\mu(\text{microchip}) = 1.2 \times T_\mu(\text{solution}) - 27.8°C \qquad \mathbf{7}$$

Correction parameters between microchip and solution plots for ΔH and ΔS may also be treated as additive constants:

$$\Delta H(\text{microchip}) = \Delta H(\text{solution}) - (24 \pm 4) \text{ kcal/mol, and} \quad \mathbf{8}$$

$$\Delta S(\text{microchip}) = \Delta S(\text{solution}) - (70 \pm 12) \text{ cal/mol} \cdot \text{K.} \quad \mathbf{9}$$

By using these relationships, several approaches for calculating thermodynamic parameters of DNA duplexes in solution (18–21) can be used to estimate the same parameters for DNA duplexes on microchips, and vice versa.

The observed decrease in the stabilities of duplexes formed on the microchips compared with the stabilities of the duplexes in solution may be attributed to the influence of both the fluorescent label and the gel substrate. By means of competitive hybridization of labeled and unlabeled oligonucleotides, it was shown that the influence of the HEX label causes a small decrease in ΔG^0, which is close to the experimental error (not shown). The 8% polyacrylamide gel used for immobilization has a 1 M concentration of amide groups. These groups are responsible for the denaturant properties of urea and formamide. Amide groups in 1 M formamide cause a decrease in ΔH by 6.4 kcal/mol for 8 bp duplexes in solution (22), although this decrease is less than that in the gel. Formamide was shown to reduce T_m more for AT-rich duplexes than for GC-rich ones (22). This is consistent with observed dependence of T_μ for immobilized oligonucleotides (Equation **7**), since the difference,

$$\Delta T_\mu = T_\mu(\text{solution}) - T_\mu(\text{microchip}) = 27.8°C - 0.2 \times T_\mu(\text{solution}) \ \mathbf{10}$$

is increasing when the value of $T_\mu(\text{solution})$ is decreasing for AT-rich duplexes.

The length and the nature of the linker between the gel and the immobilized oligonucleotides do not significantly affect duplex stability (see below and Fig. 4); other properties of the polyacrylamide gel could also be responsible for the destabilizing effect of the gel on the duplexes. It is worth mentioning that a gel in which oligonucleotides are attached through amine groups shows less of a destabilizing effect than occurs in the hydrazide crosslinking gel used here (A.Drobyshev, unpublished results), probably due to the presence of a positively charged amino group. Hydrazide crosslinked oligonucleotide microchips are less stable but easier to prepare than the amino-microchips. These microchips both have similar concentrations of immobilized oligonucleotides and are currently used by our group for different purposes.
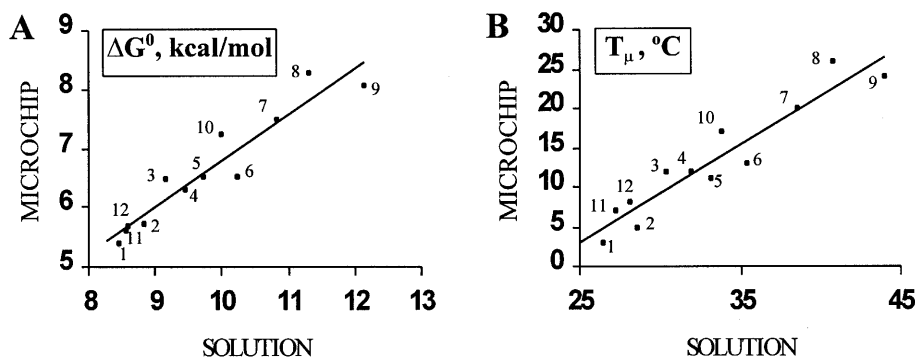
Figure 3. (**A**) Plots of free energies, ΔG^0, and (**B**) melting temperatures, T_μ, for deoxy8 bp duplexes measured on the microchips against those in solution, as determined by Doktycz *et al.* for perfect duplexes (18) and mismatched duplexes (unpublished data). Microchip nine 8 bp perfect duplexes (nos 1–9) and two duplexes containing terminal a–g, and a–a mispairs (nos 11,12) were formed by the hybridization of labeled 13mers, 5′-HEX-d(GTCCAGTCCAXYZ), in solution with immobilized deoxy8mers, 3′-gel-CAGGTX$_1$Y$_1$Z$_1$-5′. The structure of the tenth 8 bp perfect duplex, used as a control, is 5′-HEX-d(GTCCAGTCCAXYZ)/deoxy 3′-gel-CAGGTCAG-5′. The variable parts of these duplexes, 5′-XYZ-3′/3′-X$_1$Y$_1$Z$_1$-5′, have the following structures: 1) ATA/TAT, 2) AGA/TCT, 3) GAA/CTT, 4) TCA/AGT, 5) CAT/GTA, 6) TCC/AGG, 7)GGG/CCC, 8) CCG/GGC, 9) CGC/GCG, 10) GTC/CAG, 11) GAa/CTg, 12) GAa/CTa. The complementary regions in the oligonucleotides are underlined. Mispairs are marked in low cases.

Stabilization of duplexes by extension with universal bases

The shortcomings of microchips containing short oligonucleotides (6–10mers) are low stability and low hybridization signals from their duplexes. This is especially significant for 6mers. The shortcomings can be partly overcome by hybridization at low temperature, –15°C. The 100–1000 times higher capacity of the three-dimensional gel immobilization over the two-dimensional glass immobilization can also be used to increase both the hybridization signals and the duplex stabilities (2). Lengthening the immobilized oligonucleotides with the mixture of four bases (15) or a universal base that is compatible with all four DNA bases can stabilize the short duplexes without making the microchips more complex. Among several universal bases tested, such as inosine, nitropyrole and 5-nitroindole, 5-nitroindole had the best properties (14).

The immobilized oligodeoxyribonucleotides had a common core structure, 3′-XCAACCA-5′, where X = A, T, G or C. One or two 5-nitroindole-containing nucleotides were added at the 3′- or 5′-ends of the core, or the core was extended with the four-base mixture from the 3′-terminus (Fig. 4). The hybridizations and the equilibrium melting experiments were performed with the labeled oligonucleotides, 5′-AYGTTGGTAT-TMR-3′ (Y = A, G, T and C). The 5-nitroindole or four-base mixture were base paired in these duplexes with the 5′-terminal adenine. This experimental scheme allows one to estimate the effects of the terminal and penultimate base pairs on the stabilities of the duplexes containing terminal universal bases. The duplexes containing the four-base mixture included one perfect and three mismatched; however, their joint melting curves were shown to obey the standard van't Hoff equation (Equation **3**), so that the melting curves and thermodynamic parameters of such duplexes can be described using general formulas (Equations **1** and **2**). Nevertheless, no direct physical sense can be attributed to these thermodynamic parameters, which can be used only to compare total duplex stabilities. The standard free energies measured for the microchip duplexes are summarized in Figure 4.

As expected, extending the 7 bp microchip duplexes from the 3′-end by an additional base pair has a stabilizing effect. The effect is higher for the universal base (0.4–0.6 kcal/mol increase

in ΔG^0) than for the four-base mixture (0.3–0.4 kcal/mol increase in ΔG^0). The 1.36 kcal/mol rise in free energy causes the association constant of a duplex, K_a, to increase 10-fold. The stabilization only slightly depends on the penultimate base pairs (Fig. 4). The stabilization effect of the universal base or the four-base mixture at the terminal position of the duplex depends on the pairing bases, A, T, G or C. However, the difference between extreme ΔG^0 values for the different universal base pairs is <0.35 kcal/mol (Fig. 5i and j). These stabilization effects are nevertheless 0.6 kcal/mol less than that of the A–T base pair, and 1.8 kcal/mol less than that of the G–C base pair (Fig. 5g–j).

Extension of the immobilized oligonucleotides with 5-nitroindole stabilized the duplexes more efficiently from the 3′- than from the 5′-terminus (Fig. 4, compare D2 with D5 and D4 with D6). Extending the immobilized oligonucleotides with the second 5-nitroindole base from either the 3′- or 5′-end increased duplex stability, but not as much as adding the first universal base did (Fig. 4, compare D2 with D4 and D5 with D6).

As described above, the stabilities of duplexes in gel are lower than in solution. Incorporating an additional 1,2 dideoxyribose or triethylene glycol linker between a 3-methyluridine bound to the gel and a 3′-terminus of the immobilized oligonucleotide did not show any significant effect on duplex stability (Fig. 4D1 and D2).

Effect of terminal universal bases on penultimate mismatched duplex stability

The efficiency of sequencing by hybridization depends how reliable the discrimination is between perfect duplexes and duplexes containing mismatches. An internal mismatch in a short duplex destabilizes it significantly and is therefore easy to identify. However, differences in the stabilities of perfect duplexes and those containing terminal mismatches are much less prominent. The extension of the duplexes with a universal base can convert the terminal mismatches into penultimate ones. The effect of such extensions on the efficiency of discrimination was studied on oligonucleotide microchips.

The microchip contained immobilized deoxy8mers of the structure 3′-YZCAACCA-5′, where Y is 5-nitroindole, the four-base mixture, A or C; and Z = A, T, G or C. The microchip
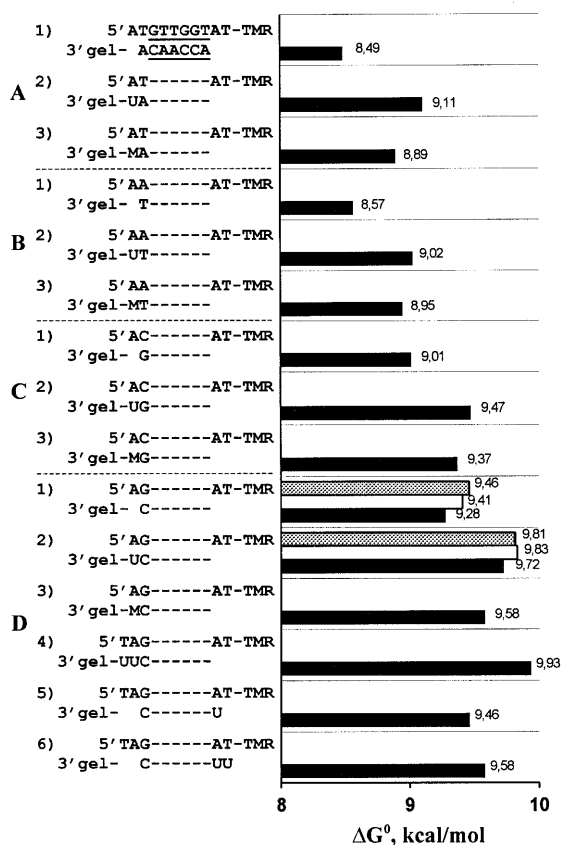
Figure 4. The stabilizing effects of linkers, the universal bases and four-base mixtures at the terminal positions of the duplexes. Free energies, ΔG^0, at 298°K were measured from equilibrium melting curves of duplexes formed by hybridization of microchip-immobilized oligonucleotides with fluorescently labeled oligonucleotides in solution. Oligonucleotides were immobilized directly through 3′-terminal 3-methyluridine (black columns) or contained an additional 1,2-dideoxyribose (white columns) and triethylene glycol (shaded columns) linkers (D1 and D2). The immobilized oligonucleotides contained the core deoxy6mer, 3′-CAACCA (A1, underlined region), extended at the 3′- or 5′-terminal position with standard and universal bases, 5-nitroindole, or the four-base mixture. The 3′-fluorescently TMR-labeled 10mers and 11mers contained 6mer core 5′-d(GTTGGT) (A1, underlined region) extended at the 5′-termini with two or three bases. The values of ΔG^0 for the duplexes are shown at the right of the bars.

Figure 5. Enhancement of the discrimination of terminal mismatches in duplexes by extension with universal base pairs. Free energies, ΔG^0, at 298°K for ten 8 bp duplexes were measured as in Figure 4. The microchip-immobilized deoxy8mers have a structure, 3′-gel-YZCAACCA-5′ (a), where Y is 5-nitroindole, the four-base mixture, A, or C and Z = A, T, G or C. The 3′-TMR-labeled 10mers have the structure d(XCGTTGGTAT) (a), where X = A, T, G or C (indicated on the ordinate). The values of ΔG^0 for the duplexes are shown at the right of the bars.

was successively hybridized with 10 fully or partly complementary 10mers of the structure 5′-XCGTTGGTAT-3′-TMR, where X = A, T, G or C. The results of the thermodynamic measurements are summarized in Figure 5. The 8 bp duplexes contained all four-base pairs with the universal base or the four-base mixture paired with A, T, G and C (Fig. 5i and j). These duplexes showed ~0.4–1.2 kcal/mol higher stabilities than those containing the terminal mismatched base pairs with C (Fig. 5g) and A (Fig. 5h). The difference increased 1–2 kcal/mol when the perfect duplexes with the terminal universal base pairs were compared with those containing penultimate mismatches C–a (Fig. 5a and b), C–t (Fig. 5c and d) and C–c (Fig. 5e and f).

These experiments show that the addition of the universal base, 5-nitroindole, or the four-base mixture to the immobilized oligonucleotides that form the terminal mismatched base pairs destabilizes the terminal mismatches by converting them into
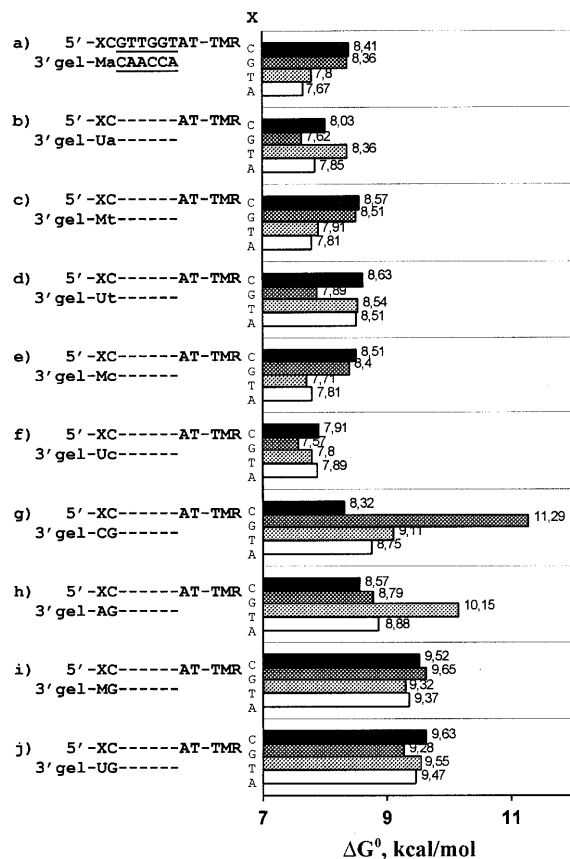
penultimate ones. This approach seems useful for enhancing discrimination of the terminal mismatches in generic oligo-nucleotide microchips.

Equalizing stabilities of AT- and GC-rich duplexes

Although not essential when the melting curves of the microchip duplexes are measured to find the optimal hybridization temperature for AT-rich and AT-poor duplexes (8), differences in stabilities of AT- and GC-rich duplexes are obstacles in sequencing by hybridization. This obstacle can also be overcome by equalizing duplex stabilities using tetramethyl ammonium (23) or betain (24) salts in the hybridization buffer, substituting some deoxyribo-nucleotides in the oligonucleotides with ribonucleotides (25), or increasing the concentration of gel-immobilized AT-rich oligo-nucleotides (2). In our studies, equalization of the duplex melting curves was carried out by extending the immobilized oligo-nucleotides with universal bases from one or both ends. Figure 6 shows a large difference in the melting temperatures for 6 bp long duplexes containing 100, 50 and 0% A-T base pairs. Extending the AT-rich duplexes from one or both ends with base pairs containing the four-base mixture diminished the difference
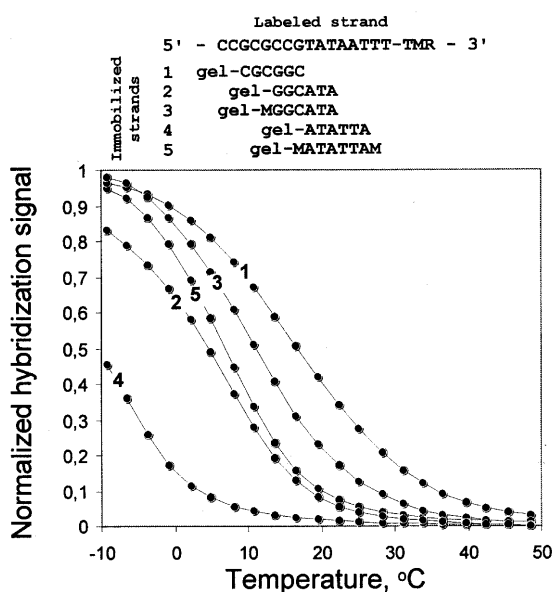
```
                    Labeled strand
        5' - CCGCGCCGTATAATTT-TMR - 3'
        1  gel-CGCGGC
        2      gel-GGCATA
        3      gel-MGGCATA
        4          gel-ATATTA
        5          gel-MATATTAM
```

Figure 6. Stabilization of AT-rich duplexes by extending them with the four-base mixture. The fluorescently labeled 16mer was hybridized with a microchip containing 100, 50 and 0% AT-rich 6mers, as such or extended from one or both ends with the four-base mixtures.

between melting temperatures for duplexes with different AT contents from 30 to 10°C. It appears that this approach can be used for constructing generic deoxy6mer microchips to equalize the stabilities of AT- and GC-rich duplexes.

CONCLUSION

MAGIChips have dual properties. They can be used as an array of immobilized compounds, or they can be used as an array of microtest tubes 70 nl or more in volume to carry out different physico-chemical processes [hybridization and fractionation, (13)], chemical reactions [oligonucleotide, DNA and protein immobilization, (6,12)] and enzymatic reactions [phosphorylation and ligation, (13)] in all or some of the gel pads.

The microchip gel pads have a high capacity for three-dimensional immobilization; therefore, microchip processes are monitored with a fluorescence microscope equipped with a CCD-camera of lower sensitivity than a laser scanner (7). This provides the advantage of measuring the kinetics of hybridization of fluorescently labeled DNA (8), non-equilibrium washing curves at a constant or gradually increased temperature (2) and the equilibrium melting curves of the duplexes in parallel and in real time of 1–2 s for all microchip-immobilized oligonucleotides. This study has used melting curve measurements to calculate the thermodynamic parameters of perfect and mismatched DNA duplexes.

Although we have carried out thermodynamic measurements for a few microchip oligonucleotides, measurements can be expanded to a much larger scale. Recently, similar measurements have been performed on a microchip containing >4000 different immobilized oligonucleotides (Mirzabekov *et al.*, unpublished results).

Such use of microchips opens new possibilities in biology and biotechnology for fast and parallel collection of an extremely large amount of experimental data. A variety of other reactions, such as enzyme–substrate, antibody–antigen, receptor–ligand and lectine–polysaccharide, could also be quantitatively studied on microchips for many compounds in parallel.

REFERENCES

1 Lysov,Y., Florentiev,V., Khorlin,A., Khrapko,K., Shik,V. and Mirzabekov,A.D. (1988) *Dokl. Acad. Nauk. SSSR* **303**, 1508–1511.
2 Khrapko,K.R., Lysov,Y.P., Khorlin,A.A., Ivanov,I.B., Yershov,G.M., Vasilenko,S.K., Florentiev,V.L. and Mirzabekov,A.D. (1991) *DNA Seq.* **1**, 375–388.
3 Southern,E.M., Maskos,U. and Elder,J.K. (1992) *Genomics* **13**, 1008–1017.
4 Fodor,S.P.A., Read,J.L., Pirrung,M.C., Stryer,L., Lu,A.T. and Solas,D. (1991) *Science* **251**, 767–773
5 Mirzabekov,A. (1994). *Trends Biotechnol.* **12**, 27–32.
6 Yershov,G., Barsky,V., Belgovskiy,A., Kirillov,E., Kreindlin,E., Ivanov,I., Parinov,S., Guschin,D., Drobishev,A., Dubiley,S. and Mirzabekov,A. (1996) *Proc. Natl. Acad. Sci. USA* **93**, 4913–4918.
7 Chee,M., Yang,R., Hubbell,E., Berno,A., Huang,X.C., Stern,D., Winkler,J., Lockhart,D.J., Morris,M.S. and Fodor,S.P.A. (1996) *Science* **274**, 610–614.
8 Drobyshev,A., Mologina,N., Shik,V., Pobedimskaya,D., Yershov,G. and Mirzabekov,A. (1997) *Gene* **188**, 45–52.
9 Lockhart,D.J., Dong,H., Byrne,M.C., Follettie,M.T., Gallo,M.V., Chee,M.S., Mittmann,M., Wang,Ch., Kobayashi,M., Horton,H. and Brown,E.L. (1996) *Nature Biotechnol.* **14**, 1675–1680.
10 Hacia,J.G., Brody,L.C., Chee,M.S., Fodor,S.P.A. and Collins,F.S. (1996) *Nature Genet.* **14**, 441–447.
11 Guschin,D.Y., Mobarry,B., Proudnikov,D., Stahl,D.A., Rittmann,B.E. and Mirzabekov,A.D. (1997) *Appl. Environ. Microbiol.* **63**, 2397–2402.
12 Guschin,D., Yershov,G., Zaslavsky,A., Gemmel,A., Shick,V., Proudnikov,D., Arenkov,P. and Mirzabekov,A. (1997) *Anal. Biochem.* **250**, 203–211.
13 Dubiley,S., Kirillov,Eu., Lysov,Yu. and Mirzabekov,A. (1997) *Nucleic Acids Res.* **25**, 2259–2265.
14 Loakes,D. and Brown,D.M. (1994) *Nucleic Acids Res.* **22**, 4039–4043.
15 Drmanac,R., Labat,I., Brukner,I. and Crkvenjakov,R. (1989) *Genomics* **4**, 114–128.
16 Timofeev,E., Kochetkova,S.V., Mirzabekov,A.D. and Florentiev,V.L. (1996) *Nucleic Acids Res.* **24**, 3142–3148.
17 Marky,L.A. and Breslauer,K.J. (1987) *Biopolymers* **26**, 1601–1620.
18 Doktycz,M.J., Morris,M.D., Dormady,S.J., Beattie,K.L. and Jacobson,K.B. (1995) *J. Biol. Chem.* **270**, 8439–8445.
19 Breslauer,K.J., Frank,R., Blocker,H. and Marky,L.A. (1986) *Proc. Natl. Acad. Sci. USA* **83**, 3746–3750.
20 Wetmur, J.G. (1991) *Crit. Rev. Biochem. Mol. Biol.* **26**, 227–259.
21 SantaLucia,J.Jr, Allawi,H.T. and Senevirante,P.A. (1996) *Biochemistry* **35**, 3555–3562.
22 Blake,R.D. and Delcourt,S.G. (1996) *Nucleic Acids Res.* **24**, 2095–2103.
23 Jacobs,K.A., Rudersdorf,R., Neill,S.D., Dougherty,J.P., Brown,E.L. and Fritsch,E.F. (1988) *Nucleic Acids Res.* **16**, 4637–4650.
24 Rees,W.A., Yager,T.D., Korte,J. and von Hippel,P.H. (1993) *Biochemistry* **32**, 137–144.
25 Hoheisel,J.D. (1996) *Nucleic Acids Res.* **24**, 430–432.